Susceptibility-induced fiber orientation dependency of the DWI signal in white matter measured in ex vivo monkey brain at 7 T

Sidsel Winther[1,2], Mariam Andersson[1,2], Henrik Lundell[2], and Tim Dyrby[1,2]

[1]*DTU Compute, Technical University of Denmark, Kongens Lyngby, Denmark,* [2]*Danish Research Centre for Magnetic Resonance, Functional and Diagnostic Imaging and Research, Copenhagen University Hospital Hvidovre, Hvidovre, Denmark*

Contact: siwin@dtu.dk

Introduction 1

Magnetic susceptibility induces morphology- and orientation-dependent perturbations of the B_0-field. At the microstructural scale of brain white matter (WM), the main contribution comes from myelin[1]. Hence, WM areas of different composition (fiber directions, dispersion, axon diameters, etc.) will be affected differently. This leads to an orientation-dependent bias. Such effects have been shown for DWI theoretically and with simulations[2,3]. We have previously shown a significant effect in simulated DWI data for straight hollow cylinders, and B-field calculations for bio-realistic axons[4] (figure 1). Here, we show similar effects in an ex vivo monkey brain.

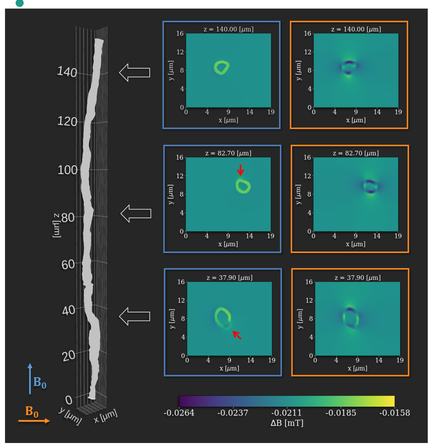

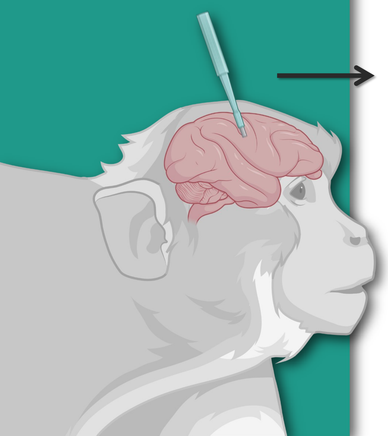

Figure 1: ***Left:*** *Axon from the CC of a vervet monkey segmented from synchrotron radiation imaging (SRI)[5].* ***Right:*** *Cross-sections of the computed perturbations ΔB of an applied field of 7 T for parallel (blue) and perpendicular (orange) orientation w.r.t. the field. Largest effect is seen for the perpendicular orientation. Gradients are stronger perpendicular to the axon than parallel to. Perturbations are non-zero for the parallel orientation (red) opposed to what is seen for the straight cylinder model.*

Methods 2

Sample: A cube was dissected from a perfusion fixated vervet monkey brain, rinsed with KPBS, and placed in the rotation device with agar (figure 2).

MRI: Bruker Biospec 70/20 7T scanner. 2D image sequence of 300 μm resolution. PGSE: δ=7.2 ms, Δ=20.2 ms, TE=36 ms, TR=3200 ms, pre-scribed b-values=(50, 1000, 2000, 3000) s/mm^2, 21 b-vectors uniformly distributed over a half-sphere (repeated with opposite polarity for cross-term correction[6] (figure 3)). Repeated at different orientations w.r.t. B_0 at θ=(0, 90, 30, 60) deg (figure 2). FOV was aligned with the longitudinal fissure at each scan.

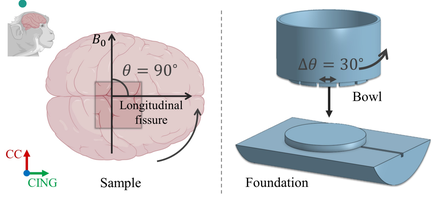

Figure 2: *Experimental setup.* ***Left:*** *A cube corresponding to the marking was dissected from a vervet monkey brain. The angle θ is the angle between the longitudinal fissure and the B_0-field. Since CC and CING are perpendicular to each other, opposite orientation dependency is expected.* ***Right:*** *The sample was placed in a rotation device; the center of the bowl is the center of the coil. The sample was moulded in agar to stabilize it in the bowl.*

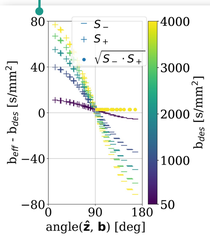

Figure 3: *Cross-term correction[6] of the effective b-values. For 2D imaging the effective b-values become skewed along the slice-direction due to the superposition of slice gradients and diffusion gradients.*

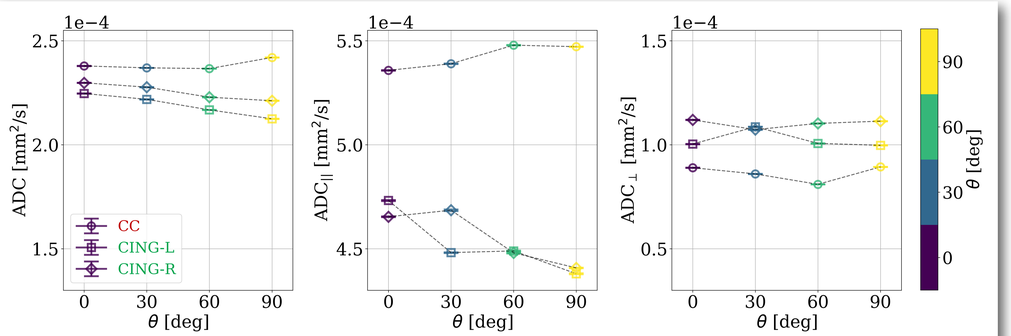

Figure 4: *A DTI model was fitted[7] to the b-values (50, 1000, 2000, 3000) s/mm^2. ADC, ADC$_{||}$, and **ADC$_\perp$** were extracted for the three ROIs: corpus callosum (CC), left cingulum (CING-L), and right cingulum (CING-R). Colour indicates at which orientation θ w.r.t. B_0 the scan was acquired. The resulting mean values and their uncertainties are plotted here. It is seen that **ADC and ADC$_{||}$ are increasing for CC while decreasing for CING. ADC$_\perp$ does not show any clear tendency.** Results from CING-L and CING-R are consistent.*

Results and discussion 3

Fiber orientation dependent effect on the DTI model.

- Statistically significant ($p<0.05$) effect of ADC and ADC$_{||}$. Not of ADC$_\perp$. Hence, anisotropic.
- For CC: ADC and ADC$_{||}$ are **in**creasing as a function of θ.
- For CING-L and CING-R: ADC and ADC$_{||}$ are **de**creasing as a function of θ.

The fiber orientation dependency is more pronounced for CING than for CC.

- This is in correspondence with the fibers of CING expressing less micro-dispersion than the fibers of CC, as we have shown previously based on synchrotron radiation imaging (SIR) of mouse brain tissue[8].
- Axon micro-dispersion is crucial for understanding these effects.

Deviations between θ=0 deg and θ=90 deg are at the order of 3-5% for ADC and ADC$_{||}$.

- This indicates that the deviations could influence axon diameter estimations[9], and cause a bias between estimations for fibers of different directions.

Why is ADC$_\perp$ not showing orientation dependency?

- Due to the stronger gradients perpendicular to axons (figure 1), we expected a stronger effect for ADC$_\perp$ compared to ADC$_{||}$.
- Could it be because ADC$_\perp$ is too low for the accumulated dephasing to affect the signal? Despite the gradients being weaker parallel to the axons, the accumulated effect could be larger in this direction due to the higher value of ADC$_{||}$.
- In our future work we will test this by running simulations on substrates with realistic micro-dispersion.

References 4

1. T. Xu, et al. *The effect of realistic geometries on the susceptibility-weighted MR signal in white matter*. Magn. Reson. Med., 2018. **2.** J. Trudeau, et al. *The Effect of Inhomogeneous Sample Susceptibility on Measured Diffusion Anisotropy Using NMR Imaging*. J. Magn. Reson. B, 1995. **3.** D. Novikov, et al. *Effects of mesoscopic susceptibility and transverse relaxation on diffusion NMR*. J. Magn. Reson., 2018. **4.** S. Winther, et al. *Orientation-dependent biases in powder averaging caused by inhomogeneous distributions of magnetic susceptibility in white matter*. ISMRM, 2020. **5.** M. Andersson, et al. *Axon morphology is modulated by the local environment and impacts the non-invasive investigation of its structure-function relationship*. PNAS, 2020. **6.** H. Jara, et al. *Determination of background gradients with diffusion MR imaging*. JMRI, 1994. **7.** E. Garyfallidis et al.. *Dipy, a library for the analysis of diffusion MRI data*. Front. Neuroinform., 2014. **8.** H. M. Kjer, et al. Streamline tractography for 3D mapping of axon bundle organization in one MRI voxel using ultra-high resolution synchrotron radiation imaging. ISMRM, 2020. **9.** M. Andersson, et al. Does powder averaging remove dispersion bias in diffusion MRI diameter estimates within real 3D axonal architectures? bioRxiv, 2021.

Some figure elements were created with BioRender.com.